Fuel 116 (2014) 388–394

Contents lists available at ScienceDirect

Fuel

journal homepage: www.elsevier.com/locate/fuel

Effect of steam injection location on syngas obtained from an air–steam gasifier

Ashokkumar M. Sharma, Ajay Kumar *, Raymond L. Huhnke

Biosystems & Agricultural Engineering Department, Oklahoma State University, Stillwater, OK 74078, USA

HIGHLIGHTS

- Studied effects of steam injection location and steam-to-biomass ratio (SBR).
- A lab-scale autothermal air–steam fluidized-bed gasifier was used for the study.
- Steam injection location and SBR had significant effects on H_2 and CO yields.
- Steam injection location had significant effects on the gasifier efficiencies.
- The best syngas yield was at the steam injection location of 254 mm and SBR of 0.2.

ARTICLE INFO

Article history:
Received 25 June 2013
Received in revised form 11 August 2013
Accepted 12 August 2013
Available online 28 August 2013

Keywords:
Fluidized-bed gasifier
Biomass
Steam port location
Syngas

ABSTRACT

For a fluidized-bed gasifier, reaction conditions vary along the height of the reactor. Hence, the steam injection location may have a considerable effect on the syngas quality. The objective of this study was to investigate the effects of steam injection location and steam-to-biomass ratio (SBR) on the syngas quality generated from an air–steam gasification of switchgrass in a 2–5 kg/h autothermal fluidized-bed gasifier. Steam injection locations of 51, 152, and 254 mm above the distributor plate and SBRs of 0.1, 0.2, and 0.3 were selected. Results showed that the syngas H_2 and CO yields were significantly influenced by the steam injection location ($p < 0.01$) and SBR ($p < 0.05$). The steam injection location also significantly influenced hot and cold gas, as well as carbon conversion efficiencies. The best syngas yields (0.018 kg H_2/kg biomass and 0.513 kg CO/kg biomass) and gasifier efficiencies (cold gas efficiency of 67%, hot gas efficiency of 72%, and carbon conversion efficiency of 96%) were at the steam injection location of 254 mm and SBR of 0.2.

1. Introduction

Dependence on fuels and chemicals derived from petroleum resources has created a major challenge to meet world's demands on a sustainable basis. Biomass is a sustainable and renewable energy resource, which has the potential to reduce a significant portion of world's dependency on petroleum resources with subsequent reduction in global warming due to greenhouse gas emissions [1–3]. Biomass gasification, a thermochemical conversion technology, is one of the promising routes for producing fuels and chemicals using biomass-derived syngas. However, synthesis of liquid fuels and chemicals using various conversion processes typically requires a syngas with a wide range of H_2/CO ratio, i.e. between 0.4 and 4 [4–8], as well as concentrations of H_2 and CO and CO_2 [8,9].

Syngas quality generated from biomass depends on several parameters such as biomass properties, gasifier design, gasifier operating conditions, and type of oxidizing agent [1]. Different gasifier designs such as downdraft, updraft, and fluidized-bed have been optimized to produce syngas having high H_2 and CO contents. Biomass properties such as size, shape, moisture content, and chemical compositions, also significantly influence syngas quality in terms of gas composition and impurities. H_2 concentration of the syngas can also be increased by optimizing the design and operating conditions of the gasifier [10]. Gasifier operating conditions such as biomass feed rate, gasification temperature, and flow rate of oxidizing agent have influence on syngas quality [1]. The biomass feed rate into the gasifier must be optimized to yield high heating value syngas with maximum energy efficiency [1]. Gasification temperature controls reactions occurring inside the reactor. A gasification temperature above 800 °C is desired to obtain high gas yield and H_2 and CO contents [1].

The type of oxidizing agent such as air, oxygen, and steam, used in biomass gasification also significantly effects quality and yield of

* Corresponding author. Tel.: +1 405 744 8396; fax: +1 405 744 6059.
E-mail address: ajay.kumar@okstate.edu (A. Kumar).

0016-2361/$ - see front matter © 2013 Elsevier Ltd. All rights reserved.
http://dx.doi.org/10.1016/j.fuel.2013.08.026

syngas. Using air as an oxidizing agent results in a syngas highly-diluted with nitrogen (up to 65%) with low heating value [11,12]. Using oxygen as an oxidizing agent results in a syngas with high CO and H_2 concentrations [13]. Using steam as an oxidizing agent results in syngas with high H_2 content [14,15]. Overall, air gasification yields a low-calorific syngas containing much less H_2 than that obtained through air–steam or steam-only gasification [11,16–18]. Air–steam gasification using fluidized bed gasifier at equivalence ratio (ER) of 0.22, steam-to-biomass ratio (SBR) of 2.7 and gasifier temperature of 900 °C resulted in syngas with a high H_2 yield (71 g/kg of biomass, wet basis) [17]. Air–steam gasification of rice hull in a fluidized bed gasifier at 800 °C showed high H_2 content (40%) in the syngas [19]. Kumar et al. (2009) studied air–steam gasification in a fluidized-bed gasifier and reported significant increase from 4% to 15% in syngas H_2 content with an increase in temperature from 650 to 850 °C [20]. Overall, air–steam gasification studies [2,17,20] showed that both steam injection and higher gasification temperatures (above 800 °C) resulted in a H_2 rich syngas, making it more suitable for further conversion into liquid fuels and chemicals.

In air–steam gasification, major reactions contributing to the high H_2 yield are water–gas and water–gas shift reactions (Eqs. (1)–(3)) [17,21]. The methane steam reforming reaction (Eq. (4)) also contributes to the H_2 content of the gas [22].

$$C + H_2O \rightarrow CO + H_2 \quad (\text{water—gas reaction}, \Delta H = 131.3\ \text{kJ/mol}) \tag{1}$$

$$C + 2H_2O \rightarrow CO_2 + 2H_2 \quad (\text{water—gas reaction}, \Delta H = 89.7\ \text{kJ/mol}) \tag{2}$$

$$CO + H_2O \rightarrow CO_2 + H_2 \quad (\text{water—gas shift reaction}, \Delta H = -41.2\ \text{kJ/mol}) \tag{3}$$

$$CH_4 + H_2O \rightarrow CO + 3H_2 \quad (\text{methane steam reforming reaction}, \Delta H = 206\ \text{kJ/mol})$$

An important consideration in maximizing efficiency and H_2 production in air–steam gasification is the location of steam injection, which can significantly affect the reaction conditions inside the gasifier. Injection of steam into a high temperature zone of the fluidized bed gasifier favors H_2 forming reactions (Eqs. (1) and (2)) and can yield H_2-rich syngas. On the contrary, injecting steam into a low temperature zone can further reduce the gasifier temperature, and thus adversely affect gasification reactions (Eqs. (1)–(3)) leading to low H_2 yield. Additionally, the formation of H_2 depends upon the residence time of reactants involved in gasification reactions. The residence time can also be optimized by changing the location of steam injection, which can further increase the H_2 content of the syngas.

Further, based on the temperature condition and carbon availability, steam injection in the reduction zone of the gasifier can increase H_2 production through reducing reactions (Eqs. (1)–(3)). In fluidized-bed gasification, drying and devolatilization of biomass occur at the bottom of the fluidized bed, which can be considered as the virtual location of both drying and pyrolysis zones. Oxidation of de-volatized products and char occur next in the middle and top of the bed, which can be considered the virtual oxidation zone. Reduction occurs in the final step of the gasification and involves conversion of pyrolysis products into syngas, and thus, the region above the combustion zone i.e. top of the bed plus the freeboard region can be considered as the virtual reduction zone. Injection of steam into the reduction zone at the top of bed and in freeboard regions may lead to high H_2 yield through reducing reactions (Eqs. (1)–(3)).

Reaction conditions vary along the height of the reactor in especially autothermal fluidized-bed gasifiers. This study is based on the hypothesis that the location of steam injection has a significant effect on syngas quality. The objective of present study was to investigate the effect of steam injection location on the quality of syngas generated from an air–steam gasification in a 2–5 kg/h autothermal lab-scale fluidized-bed gasifier.

2. Materials and methods

2.1. Biomass feedstock and bed material

All experiments were performed using Kanlow switchgrass which was grown at the Agronomy Research Station of Oklahoma State University and harvested in the fall of 2010. Proximate and ultimate analyses of switchgrass were performed by Hazen Research, Inc. (Golden, CO). A bomb calorimeter (model A1290DDEB, Parr Instrument Co., Moline, IL) was used to determine higher heating value of switchgrass (18.83 MJ per kg dry biomass). Switchgrass bales were chopped using a 25 mm screen in a Haybuster tub grinder (Model: H1000, Duratech Industries International, Inc. Jamestown, ND). Silica sand, supplied by Oglebay Norton Industrial Sands, Inc. (Brady, TX), was used as inert bed material. Bulk densities of switchgrass and silica sand were measured using a 0.0001 m^3 container. Switchgrass was poured into the container from 100 mm above the container and mass of the switchgrass in the container was determined. The bulk density was determined by dividing the mass of the switchgrass in the container with the container volume. The bulk density of silica sand was measured using the similar procedure. A digital vernier caliper (Digimatic, Mitutoyo, Japan) with 0.1 mm resolution was used to measure the particle length of switchgrass while a sieve shaker (CSC Scientific, Fairfax, VA) was used to perform particle size distribution of silica sand. The geometric mean sizes by mass of switchgrass and silica sand were determined using ANSI/ASAE Standard S319.3-February 2008 [23].

2.2. Test setup and instrumentation

Fig. 1 shows the gasifier test setup. Details of the gasifier system are described elsewhere [22]. A fluidized-bed gasifier test setup with a biomass throughput of 2–5 kg/h was used for this study. The test setup consisted of a fluidized-bed gasifier (0.1 m i.d. × 1.1 m height), a hopper, a double dump valve, a screw feeder, two cyclone separators, a producer gas burner, an air supply unit, a heat torch, and a steam boiler. The inside wall of the gasifier was thermally insulated with 1 inch refractory lining of conventional castable (Resco Products Inc., Pittsburgh, PA) while the outside wall was covered with 1 in. layer of thick cerawool (Kaowool RT Blanket-RCF-24/SW-24, Thermal Ceramics Inc. Augusta, GA). A distributor plate (0.28 m o.d. × 5 mm thickness) was located at the bottom of the gasifier to uniformly distribute the inlet air, and to support a bed of silica sand. A 30 × 30 mesh size wire screen was placed on the top of the distributor plate to prevent the silica sand from falling down through the distributor plate. The biomass hopper was fitted with a stirrer to prevent bridging of the biomass feedstock and a screw coupled with a 90 V DC motor (Model: 2M168D, Dayton Electric Mfg. Co., Niles, IL) at the bottom for discharging biomass to the gasifier screw feeder. A DC speed regulator (Model: 4Z829B, Dayton Electric Mfg. Co., Niles, IL) was used with the gasifier screw motor to control the biomass flow rate into the gasifier. A double dump valve (Fig. 1) between the hopper exit and screw feeder was used to isolate the hopper from the gasifier and thus prevented backflow of hot gases into the biomass hopper. Two cyclone separators were connected in series to remove partic-

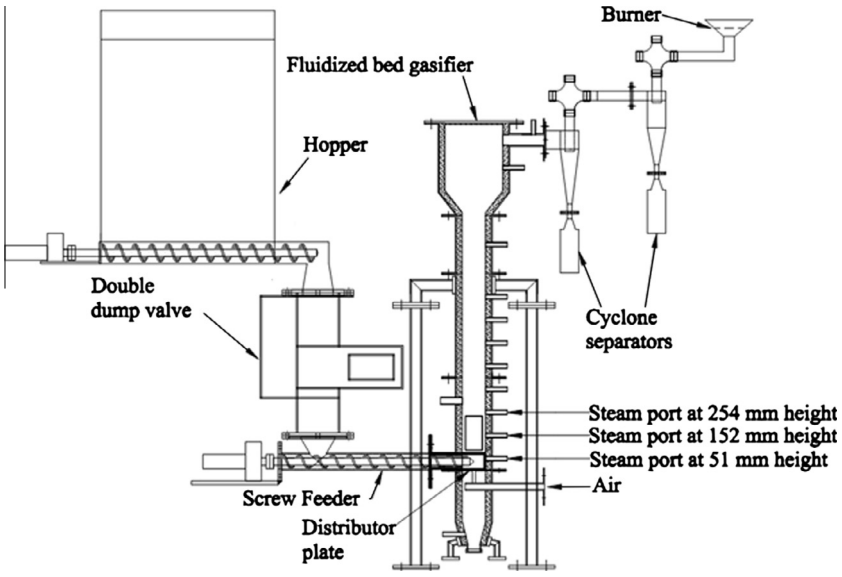

Fig. 1. Gasification test setup. Note that three steam injection locations were in the bottom, middle and top of the fluidized bed of the gasifier.

ulates from the gas at the gasifier exit. A burner at the end of the gas pipe lines was used to combust the exiting gas.

Air was supplied using an air compressor (Model: TS10K10, Ingersoll Rand, Davidson, NC). An air control valve, mass flow meter (Model: 8059MPNH, Eldridge Products, Inc., Monterey, CA), and pressure regulator (Model: 4Zk96, Grainger, Inc., Oklahoma City, OK) were fitted in-line with the air supply line. A heat torch (Model: HT200, Farnam Custom Products, CA) was used to heat air for preheating the sand bed inside the gasifier. A steam boiler (Model: MBA12, Sussman Electric Boilers, NY) was used to inject the steam into the gasifier. A stainless steel tube coil (8 mm i.d.) wrapped with a heat tape (Model: SRT051-040, Omega Engineering, Inc., Stamford, CT) was used to superheat the steam. A mass flow meter (Model: 1/2-73-R-101-HR-ESK, RCM Industries, Inc., CA) and flow control ball valve were used at the boiler outlet to monitor and control the steam flow rate. A U-tube water manometer and a differential pressure transducer (Model: PX154-025DI, Omega Engineering, Inc., Stamford, CT) were used to measure pressure drop across the gasifier. Sampling ports were available in the gas pipe line for taking samples of syngas, tar and particulates. Gas pipe lines were wrapped with heat tapes for maintaining pipe line temperature above 300 °C to prevent condensation of tars and water vapor. Gasifier operation was monitored using a LabVIEW system (National Instruments, Austin, TX).

2.3. Experimental design

A total of 18 gasification experiments (3 locations × 3 SBRs × 2 replications) were performed at ER of 0.32. The ER of 0.32 was selected for this study based on our earlier study with the 2–5 kg/h autothermal lab-scale fluidized bed gasifier that concluded that ER of 0.32 was optimum to obtain the best syngas composition, gas heating value, and gasifier energy efficiency [22]. The gasifier reactor temperature varied along the height of the reactor at the ER of 0.32, (shown in Table 1). Based on the gasifier temperature, three gasifier locations at the heights of 51 mm, 152 mm, and 254 mm above the distributor plate were selected for steam injection. SBR was selected between 0.1 and 0.3 (maximum) based on our preliminary experiments to maintain autothermal requirements of the gasifier reactor.

Table 1
Reactor temperature along the height of the gasifier at ER = 0.32.

Location above distributor plate (mm)	Average temperature (°C)
51	880
152	755
254	524
Above 356	⩽340

2.4. Test procedure and system maintenance

A small inspection window (102 mm × 152 mm) with an air-tight door was provided on the gasifier wall above the distributor plate for loading the sand in the gasifier and for maintenance work. 1.5 kg of sand was placed on the distributor plate through the inspection window and then the window was properly sealed. A thin cerawool packing and a high temperature RED RTV silicone gel (Type 650, Versachem, Riviera Beach, FL) were used to make metal flanges air-tight. Initially, the sand bed was preheated to 400 °C by supplying hot air using the heat torch. The bed temperature was further raised to 700 °C by feeding a low quantity of biomass into the gasifier. Typically, 20–40 min after the preheating, the gasifier temperature profile became uniform and the gas burner showed consistent flame from the exiting gas. The heat torch was then extinguished, and the gasification conditions such as flow rates of air and biomass were adjusted to desired levels as per experimental design. Steam was then injected into the gasifier at the specified location. Duration of each test run was between 2 and 3 h.

System maintenance was performed the following day after each test run. During maintenance, the entire gasifier reactor, gas pipe lines, cyclone separators, and the burner were properly cleaned to remove any remaining tars and particulates. Used sand was removed using a vacuum cleaner through inspection window located at the gasifier bottom. After cleaning, the setup was prepared for the next test run. Unused biomass was also removed from the hopper, and the hopper was filled with a fresh biomass for the next test run.

2.5. Measurements and calculations

All data measurements were recorded when the gasifier temperature profile was stable, and the exiting gas was flammable.

Flow rates of air, biomass, and steam; temperature of gasifier; gas-exit; gas-flame and steam; and pressure drop across the gasifier were continuously monitored. LabVIEW software was used for continuous recording of temperatures, pressure drop and air flow rate. Air and biomass flow rates were controlled using the LabVIEW program. To determine biomass flow rate, a calibration was performed between biomass flow rate and motor speed. The steam flow rate was measured using the steam mass flow meter. Equipment details and measurement techniques used for sampling gas, tar, and particulates, and gas and tar analyses are described elsewhere [22]. Equations to determine gas yield, gas heating value and gasifier efficiencies, i.e. cold gas, hot gas, and carbon conversion efficiencies, were used from literature [22]. Statistical analysis was performed using statistical software SAS (Release 9.3, SAS, Cary, NC, USA). Analysis of variance (ANOVA) method with generalized linear model (GLM) procedure was used to study effects of steam injection port location and SBR (independent variables) on syngas yield, concentrations and impurities, gasification temperature, and gasifier efficiencies (dependent variables). The alpha (level of significance) for the statistical analysis was held constant at 0.05.

3. Results and discussion

Air–steam gasification of switchgrass was performed using the lab-scale fluidized-bed gasifier to study the effects of steam injection port location and SBR on the gasifier performance. Biomass properties, gas composition and heating value, tar and particulate contents, as well as gasifier efficiencies, are discussed in the following subsections.

3.1. Biomass characteristics

Proximate and ultimate analyses of the Kanlow switchgrass are shown in Table 2. Bulk densities of chopped switchgrass and silica sand ranged from 105 to 117 kg/m^3 and 1592 to 1612 kg/m^3, respectively. Particle geometric mean size by mass of chopped switchgrass and silica sand were calculated to be 10 ± 1.7 mm and 336 ± 2 μm, respectively.

3.2. Gasifier temperature

The effect of SBR on the gasification temperature at the three steam injection port locations, i.e. 51, 152 and 254 mm, is shown in Fig. 2. The average temperature of steam at injection was 201 °C, which was lower than the normal operating temperature of the gasifier bed (Table 1). Therefore, the steam injection into the gasifier caused quenching of the temperature environment at all injection locations leading to decrease in gasification temperature. Additionally, the quantity of steam injected into the gasifier increased with SBR, which directly influenced the gasifier temperature, resulting in further decreases in the temperature of the reactor bed. As a consequence, the gasifier temperature decreased with an increase in the SBR from 0.0 to 0.3 as shown in Fig. 2. The gasifier temperature decreased with increase in SBR at all steam injection port locations. At steam injection port location of 51 mm, with an increase in SBR, the gasifier temperature decreased from 713 °C at SBR of 0.1 to 419 °C at SBR of 0.2, and 367 °C at SBR of 0.3. Similarly, at steam injection port location of 152 mm, the gasifier temperature decreased from 549 °C at SBR of 0.1 to 437 °C at SBR of 0.2, and 482 °C at SBR of 0.3. At steam injection port location of 254 mm, with an increase in SBR, the gasifier temperature decreased from 664 °C at SBR of 0.1 to 636 °C at SBR of 0.2, and 587 °C at SBR of 0.3. At steam injection port locations of 51 and 152 mm, the increase in the SBR from 0.1 to 0.3 significantly decreased ($p < 0.05$) the gasification temperature by 104–449 °C (Fig. 2). This is primarily attributed to the quenching of the dense phase of bed materials at the lowest and middle, steam injection port positions. At steam injection port location of 254 mm, with an increase in SBR, the gasifier temperature decreased from 664 °C at SBR of 0.1 to 636 °C at SBR of 0.2, and 587 °C at SBR of 0.3. The 254 mm steam injection port was located at the top of the bed that included a lean phase of the bed materials. As a result, the increase in the SBR from 0.1 to 0.3 did not show a significant influence on the gasification temperatures at 254 mm steam injection port location (shown in Fig. 2).

Table 2
Material properties.

Proximate analysis (wt.%, d.b.)[a]		Ultimate analysis (wt.%, daf) [b]	
Moisture content	14.63	Carbon	52.74
Ash content	4.72	Hydrogen	5.91
Fixed carbon	13.69	Oxygen	41.05
Volatile matter	81.59	Nitrogen	0.24
		Sulfur	0.06

[a] Dry basis.
[b] Dry ash-free.

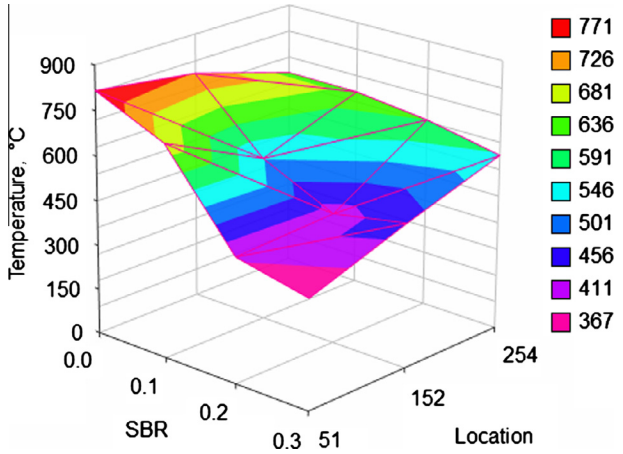

Fig. 2. Gasifier temperature with varying steam injection port location and SBR.

3.3. Gas composition

CO and H_2 yields in syngas are influenced by the gasification temperature and the availability of limited reactant (H_2O). The water–gas reaction (Eq. (1)) that yields both H_2 and CO is an endothermic reaction, i.e. $\Delta H > 0$, and is considerably influenced by the gasification temperature [24]. Thermodynamically, higher gasification temperatures favor endothermic gasification reactions such as (Eq. (1)) resulting in more H_2 and CO. Also, in addition to gasification temperatures, the quantity of limiting reactant, i.e. H_2O, considerably influences the production of H_2 and CO through water gas reaction (Eq. (1)). This is because at higher levels of limiting reactant (H_2O), more H_2O reacts with the available carbon to form H_2, CO, and CO_2 through reactions (Eqs. (1) and (2)).

In the present study, the maximum H_2O was available at SBR of 0.3. Hence, it was anticipated that the SBR of 0.3 would result maximum H_2 and CO yields through reaction (Eq. (1)). However, as explained above, due to a significant decrease in the gasification temperature at the 51 and 152 mm steam injection port locations, the SBR of 0.3 resulted in lower H_2 (Fig. 3) and CO (Fig. 4) yields. Also, the decrease in the gasification temperature caused reduction in the gas volumetric flowrate (due to cooling effect) through the bed materials resulting in decrease of overall bed-expansion and turbulence level in the fluidized-bed [25,26]. Such a decrease in the bed expansion and in-bed turbulence level may have further

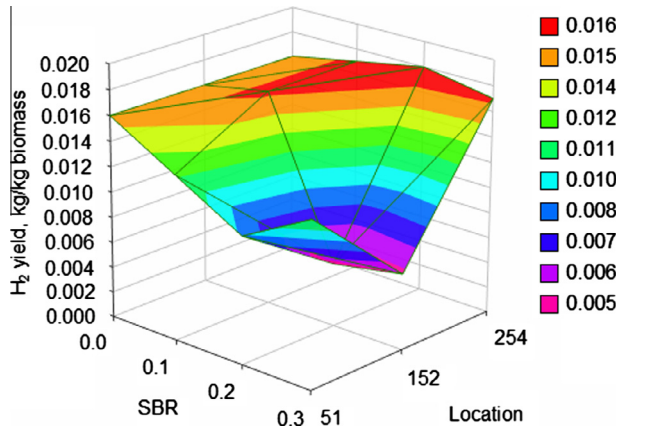

Fig. 3. Syngas hydrogen yield with varying steam injection port location and SBR.

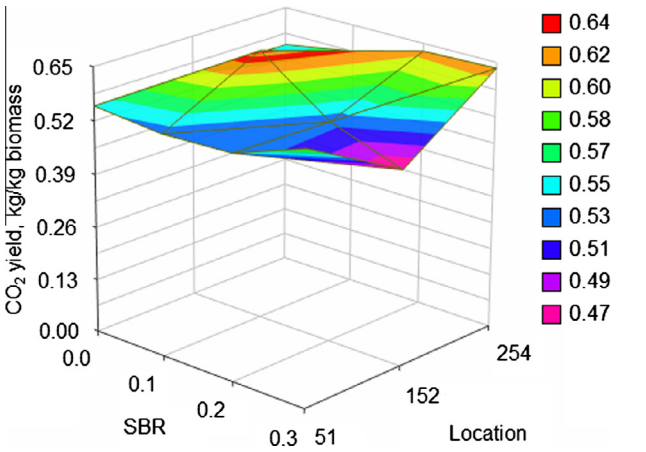

Fig. 5. Syngas carbon dioxide yield with varying steam injection port location and SBR.

reduced the overall heat and mass transfer in the gasifier bed, resulting in the lower H_2 and CO yields at steam injection port locations of 51 and 152 mm.

At the 254 mm steam injection port location, maximum CO and H_2 yields were observed at SBR of 0.2. The SBR of 0.3 showed 4% and 17% lower H_2 and CO yields, respectively, than at SBR of 0.2. Such observations can be explained by the decrease in the gasification temperature (Fig. 2) caused by the higher steam injection at SBR of 0.3. Also, at 254 mm steam injection port location, the SBR of 0.1 resulted in 5% and 13% lower H_2 and CO yields, respectively, than those at SBR of 0.2. No steam injection (SBR of 0.0) also resulted in lower CO and H_2 yields than those obtained at SBR of 0.2. It can be inferred from these results that SBR of 0.2 at steam injection of 254 mm provided the best combination of bed temperature and H_2O to maximize CO and H_2 yields. Results show that steam injection at the 254 mm port (located in the reduction zone of the gasifier) led to high H_2 yield. The high H_2 yield can be attributed to reducing reactions (Eqs. (1)–(3)), as discussed earlier.

Water–gas shift reaction (Eq. (3)) is also an important gasification reaction that produces H_2. However, this reaction also increases CO_2 yield. High CO_2 yields at steam injection port location of 254 mm (Fig. 5) can be attributed to the water–gas shift reaction (Eq. (3)) that also contributed to the high H_2 yield. Alternatively, the high CO_2 yields can be attributed to the reaction (Eq. (2)) leading to the consumption of injected H_2O (steam), producing H_2 as well as CO_2. The endothermic methane steam reforming reaction (Eq. (4)) could also have contributed to the high H_2 and

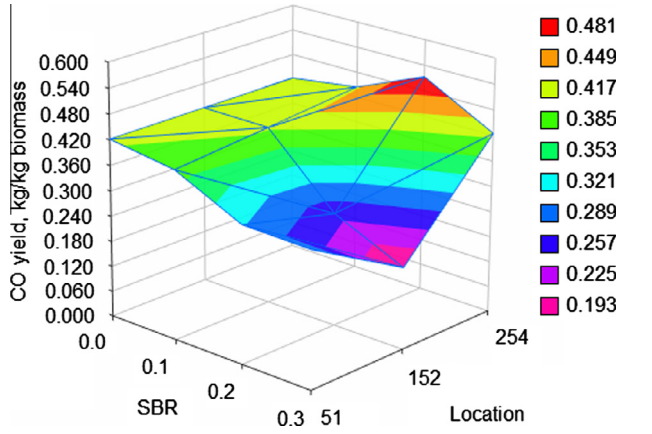

Fig. 4. Syngas carbon monoxide yield with varying steam injection port location and SBR.

CO yields at the steam injection port location of 254 mm. This was because at high gasification temperatures, as observed at this location and in the presence of H_2O, methane is less thermodynamically stable and could have converted to more stable gaseous products, i.e. H_2 and CO.

Statistical results showed that both steam injection port location ($p < 0.01$) and SBR ($p < 0.05$) had highly significant effects on H_2 and CO yields. Also, the interaction between steam injection port location and SBR was significant ($p < 0.05$). The effect of steam injection port location and SBR on the syngas CO_2 yield was, however, not significant. Overall, the SBR of 0.2 and steam injection port location of 254 mm resulted in 12% and 18% higher syngas H_2 and CO yields, respectively, than H_2 and CO yields obtained without any steam injection.

Concentrations of CO, H_2, CO_2, CH_4 and N_2 in syngas depend on several factors such as gasification temperature and quantities of limiting reactants (H_2O and O_2). In the present study, concentrations of H_2, CO, CO_2, CH_4 and N_2 with no steam injection (at SBR of 0.0) were 8.4%, 16.4%, 13.7%, 2.3% and 57.8%, respectively. Steam injection at 51 mm port location decreased H_2, CO and CH_4 concentrations as shown in Fig. 6(a). The reduction in H_2, CO and CH_4 concentrations was mainly due to decrease in gasification temperature with steam injection at the 51 mm port. However, with the steam injection, CO_2 content was found to increase (by 2–17%). The N_2 content was mainly dependent on the quantity of air supplied to the gasifier. Since ER in the present study was held constant at 0.32, the syngas N_2 concentration followed an opposite trend with the cumulative concentrations of H_2, CO, CO_2 and CH_4. The N_2 concentration increased (by 1–10%) with an increase in SBR.

At steam port location of 152 mm, syngas H_2 concentration increased by 6% at SBR of 0.1 as compared to that with no steam injection. However, with further increase in steam injection at SBR of 0.2 and 0.3, H2 concentration considerably decreased by 52–62%. With increase in SBR, CO and CH_4 concentrations continue to decrease by 3–43% and 20–47%, respectively, as compared to those obtained with no steam injection. On the contrary, CO_2 concentration increased by 6–15% with an increase in SBR. The N_2 concentration decreased slightly (4%) at SBR of 0.1 as compared to that with no steam injection and then increased (16–17%) at SBRs above 0.1.

At steam port location of 254 mm, the gasification temperature was not significantly affected by SBR. Further 254 mm steam injection port location and at SBR of 0.2 showed the maximum H_2 (9.0%) and CO (18.7%) concentrations. This implies that the 254 mm port location and the SBR of 0.2 provided the best combination of bed

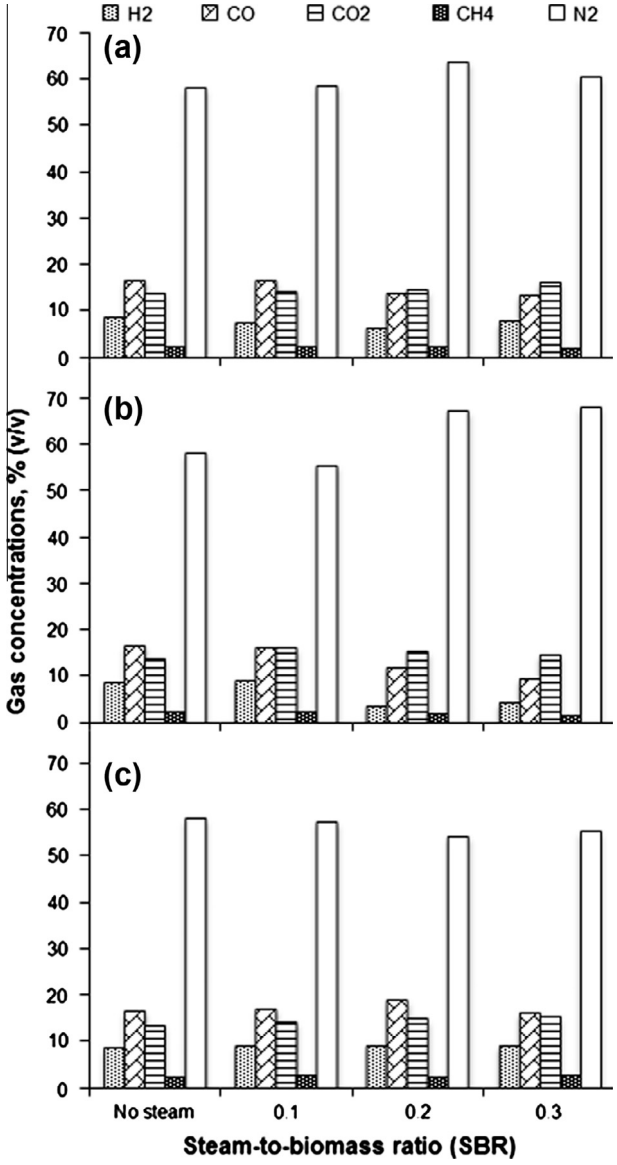

Fig. 6. Concentrations of syngas with varying SBR at different steam injection port locations. (a) 51 mm, (b) 152 mm, and (c) 254 mm.

temperature and H_2O to produce CO and H_2. H_2 concentration increased by 4–7% with an increase in SBR compared to that with no steam injection. CO concentration also increased by 2–14% with an increase in SBR from 0.1 to 0.2 while it decreased by 3% with further increase in SBR from 0.2 to 0.3 (Fig. 6(c)). The CH_4 concentration remained constant at SBRs of 0.1 and 0.3; however, it decreased by 7% at SBR of 0.2 as compared to that obtained with no steam injection. The decrease in the CH_4 and increase in CO and H_2 concentrations indicate that methane steam reforming reaction (Eq. (4)) may have occurred. The CO_2 concentration increased by 3–10% with an increase in SBR as compared to that obtained with no steam injection. The N_2 concentration decreased by 1–7% with an increase in SBR as compared to that obtained with no steam injection. The decrease in N_2 concentration was mainly due to the increase in CO, H_2 and CO_2 concentrations as discussed above. Statistical analysis showed that syngas CO and H_2 concentrations were significantly influenced by the steam injection port location ($p < 0.01$) and SBR ($p < 0.05$). However, the interaction effect of steam injection port location and SBR on the syngas CO_2 concentration was not significant.

3.4. Syngas yield, heating value and impurities

Syngas yield, which is the quantity of gas produced (Nm^3) per kg of dry biomass, depends primarily on gasification temperature and quantities of reacting species, i.e. biomass, air, and steam supplied to the gasifier. Since quantities of biomass and air were held constant, gasification temperature and SBR were the variables that influenced the syngas yield. With an increase in SBR from 0.1 to 0.3, higher gasification temperatures were observed at the 254 mm steam injection port location (Fig. 2). Further, the maximum quantity of steam injected into the gasifier was at SBR of 0.3; however, SBR of 0.3 resulted in a decrease in the gasification temperature at 254 mm steam injection port location, and thus, showed lower syngas yield (2.14 Nm^3 per kg of dry biomass). The maximum syngas yield of 2.19 Nm^3 per kg of dry biomass was observed at SBR of 0.2 at the 254 mm steam injection port location.

Syngas heating value depends upon concentrations of primary combustible products, i.e. H_2 and CO. The other minor constituents of the syngas were the lighter hydrocarbons, i.e. CH_4, C_2H_2, C_2H_4 and C_2H_6 that also contain considerable amounts of energy and have influence on the syngas heating value. In the present study for all gasification conditions, the syngas heating value ranged between 3.3 and 5.4 MJ/Nm^3. The 254 mm steam injection port location and SBR of 0.2 resulted in the highest syngas H_2 (9.0%) and CO (18.7%) contents leading to the maximum syngas heating of 5.4 MJ/Nm^3.

Tar and particulate contents are the major impurities in the syngas. Tar, a condensable organic compound, is composed of several hydrocarbons heavier than benzene and its quantity in syngas mainly depends on biomass properties, and gasification conditions such as temperature and residence time. Steam injection can reform tar leading to an overall reduction in tar. In the present study, the maximum tar content of 29.5 g/Nm^3 was observed at the 152 mm steam injection port and SBR of 0.3. At 152 mm steam injection port, the tar content increased from 18.8 to 29.5 g/Nm^3 with an increase in SBR from 0.1 to 0.3. The increase in tar content with increased SBR can be attributed to quenching of devolatilized products within the gasifier bed by the low temperature steam, as explained earlier. However, steam injections at 51 and 254 mm port locations showed low syngas tar contents (1.9–8.1 and 4.1–18.5 g/Nm^3, respectively) implying that the injected steam participated in tar-reforming reactions leading to decrease in the overall tar content. The maximum particulate content of 12 g/Nm^3 was observed at the 152 mm steam injection port location and the SBR of 0.3. Statistical results showed that both tar and particulate contents were not significantly influenced by either the steam injection port location or SBR.

3.5. Gasifier efficiencies

The gasifier cold gas and hot gas efficiencies depend on the syngas heating value and yield. The hot gas efficiency also depends on sensible energy content of the syngas, which is directly proportional to the syngas exit temperature. Statistical analysis showed that the steam injection port location had a significant effect on the cold gas and hot gas efficiencies ($p < 0.05$) while SBR showed a significant effect ($p < 0.05$) on only the hot gas efficiency of the gasifier. As explained earlier, the decrease in the gasification temperature at the steam injection port locations of 51 and 152 mm resulted in the lower syngas exit temperature, which in turn decreased the hot gas efficiency at steam injection port locations below 254 mm. The 254 mm steam injection port location and SBR of 0.2 resulted in the maximum cold gas (67%) and hot gas (72%) efficiencies (Fig. 7).

Carbon conversion efficiency of the gasifier depends on the concentrations of carbon containing gaseous products of the syngas

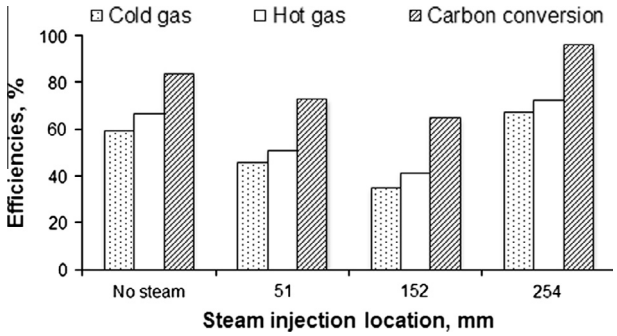

Fig. 7. Gasifier efficiencies at three steam injection port locations at SBR of 0.2.

such as CO, CO_2 and other lighter hydrocarbons. The maximum carbon conversion efficiency of 96% was observed at the 254 mm steam injection port location and SBR of 0.2. Statistical results showed that the steam injection port location had a highly significant influence ($p < 0.01$) on the carbon conversion efficiency. The interaction between steam injection port location and SBR (location*SBR) had significant influence ($p < 0.05$) on the carbon conversion efficiency. However, the effect of SBR alone on the carbon conversion efficiency was not significant.

4. Conclusion

Air–steam gasification of switchgrass was performed using an autothermal lab-scale fluidized-bed gasifier to investigate the effects of steam injection port location and steam-to-biomass ratio (SBR) on syngas composition, yield and impurities, as well as, gasifier efficiencies. Statistical results showed that the syngas H_2 and CO yields were significantly influenced by the steam injection port location ($p < 0.01$) and SBR ($p < 0.05$). The steam injection port location had also significant effect ($p < 0.05$) on the gasifier cold gas and hot gas efficiencies. However, SBR had significant effect on the hot gas efficiency but not on the cold gas efficiency. The carbon conversion efficiency was significantly influenced ($p < 0.01$) by the steam injection port location but not by the SBR. The 254 mm steam injection port location and SBR of 0.2 resulted in the maximum syngas H_2 (0.018 kg/dry kg biomass) and CO (0.513 kg/dry kg biomass) yields, cold gas (67%), hot gas (72%) and carbon conversion (96%) efficiencies.

Acknowledgements

This work was supported in part by NSF-EPSCoR award EPS-0814361 and the Director of the Oklahoma Agricultural Experiment Station. The authors also acknowledge the support of graduate students Karthikragunath Mariyappan, Nitesh Rentam and Mohit Dobhal for assisting with the experimental work.

References

[1] Kumar A, Jones DD, Hanna MA. Thermochemical biomass gasification: a review of the current status of the technology. Energies 2009;2:556–81.
[2] Lv P, Xiong Z, Chang J, Wu C, Chen Y, Zhu J. An experimental study on biomass air–steam gasification in a fluidized bed. Bioresource Technol 2004;95:95–101.
[3] Schuster G, Löffler G, Weigl K, Hofbauer H. Biomass steam gasification–an extensive parametric modeling study. Bioresource Technol 2001;77:71–9.
[4] Hamelinck CN, Faaij APC. Future prospects for production of methanol and hydrogen from biomass. J Power Sources 2002;111:1–22.
[5] Jess A, Popp R, Hedden K. Fischer-Tropsch-synthesis with nitrogen-rich syngas – fundamentals and reactor design aspects. Appl Catal a-Gen 1999;186:321–42.
[6] Klasson KT, Ackerson MD, Clausen EC, Gaddy JL. Biological conversion of coal and coal-derived synthesis gas. Fuel 1993;72:1673–8.
[7] Spath PL, Dayton DC. Preliminary screening – technical and economic assessment of synthesis gas to fuels and chemicals with emphasis on the potential for biomass-derived syngas. NREL; 2003.
[8] Wender I. Reactions of synthesis gas. Fuel Process Technol 1996;48:189–297.
[9] Zhang W. Automotive fuels from biomass via gasification. Fuel Process Technol 2010;91:866–76.
[10] Cox JL, Tonkovich AY, Elliott DC, Baker EG, Hoffman EJ. In: Second biomass conference of the Americans: energy, environment, agriculture, and industry proceeding; National Renewable Energy Laboratory, Golden, CO; 1995. p. 657–74.
[11] Delgado J, Aznar MP, Corella J. Biomass gasification with steam in fluidized bed: Effectiveness of CaO, MgO, and CaO–MgO for hot raw gas cleaning. Ind Eng Chem Res 1997;36:1535–43.
[12] Seo MW, Goo JH, Kim SD, Lee SH, Choi YC. Gasification characteristics of coal/biomass blend in a dual circulating fluidized bed reactor. Energy Fuel 2010;24:3108–18.
[13] Zhou J, Chen Q, Zhao H, Cao X, Mei Q, Luo Z, et al. Biomass–oxygen gasification in a high-temperature entrained-flow gasifier. Biotechnol Adv 2009;27:606–11.
[14] Bridgwater T. Biomass for energy. J Sci Food Agr 2006;86:1755–68.
[15] Weerachanchai P, Horio M, Tangsathitkulchai C. Effects of gasifying conditions and bed materials on fluidized bed steam gasification of wood biomass. Biores Technol 2009;100:1419–27.
[16] Baratieri M, Baggio P, Fiori L, Grigiante M. Biomass as an energy source: thermodynamic constraints on the performance of the conversion process. Bioresource Technol 2008;99:7063–73.
[17] Lv P, Chang J, Xiong Z, Huang H, Wu C, Chen Y, et al. Biomass air–steam gasification in a fluidized bed to produce hydrogen-rich gas. Energy Fuels 2003;17:677–82.
[18] Ross D, Noda R, Horio M, Kosminski A, Ashman P, Mullinger P. Axial gas profiles in a bubbling fluidised bed biomass gasifier. Fuel 2007;86:1417–29.
[19] Boateng A, Walawender W, Fan L, Chee C. Fluidized-bed steam gasification of rice hull. Bioresource Technol 1992;40:235–9.
[20] Kumar A, Eskridge K, Jones DD, Hanna MA. Steam-air fluidized bed gasification of distillers grains: Effects of steam to biomass ratio, equivalence ratio and gasification temperature. Bioresource Technol 2009;100:2062–8.
[21] Wang Y, Yoshikawa K, Namioka T, Hashimoto Y. Performance optimization of two-staged gasification system for woody biomass. Fuel Process Technol 2007;88:243–50.
[22] Sharma AM, Kumar A, Patil KN, Huhmke RL. Performance evaluation of a lab-scale fluidized bed gasifier using switchgrass as feedstock. Trans ASABE 2011;56:2259–66.
[23] ASABE-Standards. ANSI/ASAE S319. 3 February 2008: Method of determining and expressing fineness of feed materials by sieving. ASABE. St. Joseph, Mich; 1997.
[24] Franco C, Pinto F, Gulyurtlu I, Cabrita I. The study of reactions influencing the biomass steam gasification process. Fuel 2003;82:835–42.
[25] Sharma AM, Kumar A, Patil KN, Huhnke RL. Fluidization characteristics of a mixture of gasifier solid residues, switchgrass and inert material. Powder Technol 2013;235:661–8.
[26] Daleffe RV, Ferreira MC, Freire JT. Effects of binary particle size distribution on the fluid dynamic behavior of fluidized, vibrated and vibrofluidized beds. Braz J Chem Eng 2008;25:83–94.